



Multiple scattering of polarized light by particles in an absorbing medium

MICHAEL I. MISHCHENKO^{1,*}  AND JANNA M. DLUGACH²

¹NASA Goddard Institute for Space Studies, 2880 Broadway, New York, New York 10025, USA

²Main Astronomical Observatory of the National Academy of Sciences of Ukraine, 27 Zabolotny Str., 03143, Kyiv, Ukraine

*Corresponding author: michael.i.mishchenko@nasa.gov

Received 6 May 2019; revised 22 May 2019; accepted 22 May 2019; posted 23 May 2019 (Doc. ID 366865); published 13 June 2019

We study multiple scattering of light by particles embedded in an absorbing host medium using a recently developed single-scattering and vector radiative-transfer methodology directly based on the Maxwell equations. The first-principles results are compared with those rendered by the conventional heuristic approach according to which the single-scattering properties of particles can be computed by assuming that the host medium is nonabsorbing. Our analysis shows that the conventional approach yields very accurate results in the case of aerosol and cloud particles suspended in an absorbing gaseous atmosphere. In the case of air bubbles in water, the traditional approach can cause large relative errors in reflectance, but only when strong absorption in the host medium makes the resulting reflectance very small. The corresponding polarization errors are substantially smaller. © 2019 Optical Society of America

<https://doi.org/10.1364/AO.58.004871>

1. INTRODUCTION

The conventional theory of electromagnetic scattering by particles traditionally used in many applied disciplines, including those of remote sensing and atmospheric radiation, is based on the assumption that the host medium surrounding the particles is perfectly nonabsorbing, i.e., that the imaginary part m_1'' of the corresponding refractive index is precisely equal to zero (e.g., Refs. [1–24] and numerous references therein). However, natural and artificial water bodies (including oceanic whitecaps [25]) and layers of ice are but just two ubiquitous examples of absorbing host media with an imaginary part of the refractive index deviating substantially from zero at infrared wavelengths [26,27]. Another prime example of a host medium with $m_1'' \neq 0$ is the terrestrial gaseous atmosphere at wavelengths within strong absorption bands caused by components such as H₂O, O₂, and CO₂. Of course, many more examples of absorbing host media containing particles can be given.

It has been argued extensively (e.g., [28–49]) that conventional theory cannot be used to compute single and multiple light scattering by particles hosted by a medium with $m_1'' \neq 0$ and must be replaced by a more general theory. However, for a long time there had been no consensus as to how to generalize the standard notion of the optical cross sections and reformulate the conventional radiative transfer equation (RTE). It is clear that the best way to resolve this persisting uncertainty is to replace speculative arguments with a straightforward derivation directly from the Maxwell equations. Significant progress in this direction has been achieved and reported in [50–54].

Based on the first-principles modeling tools described in [53,54], it has been shown that the effects of increasing m_1'' on single scattering by an isolated spherical particle can be quite profound and can result in unexpected optical phenomena such as negative extinction [55,56]. Yet multiple scattering by a cloud of particles entails long propagation paths that can contribute virtually nothing to the signal measured by an external detector of light if absorption in the host medium is sufficiently strong. It is therefore essential to analyze whether the effects of increasing m_1'' on single scattering can manifest themselves in multiple scattering before m_1'' becomes so large that the entire particulate medium starts to appear essentially black. We will do that in the rest of this paper using the single-scattering and radiative-transfer modeling tools described in [52–54,57]. Unlike in [49], we will solve the RTE with full account of polarization instead of resorting to the scalar approximation and will assume particle volume densities sufficiently small to be in the purview of radiative transfer theory.

2. STATEMENT OF PROBLEM

The generalized RTE describing multiple scattering of polarized light by a large, sparse, and random multiparticle group was derived in [52] under the assumption that the absorbing host medium is unbounded. In our analysis, we will assume that the generalized RTE remains valid in application to a simple scattering model in the form of particles randomly and sparsely distributed throughout a plane-parallel layer of a homogeneous absorbing medium surrounded by a vacuum

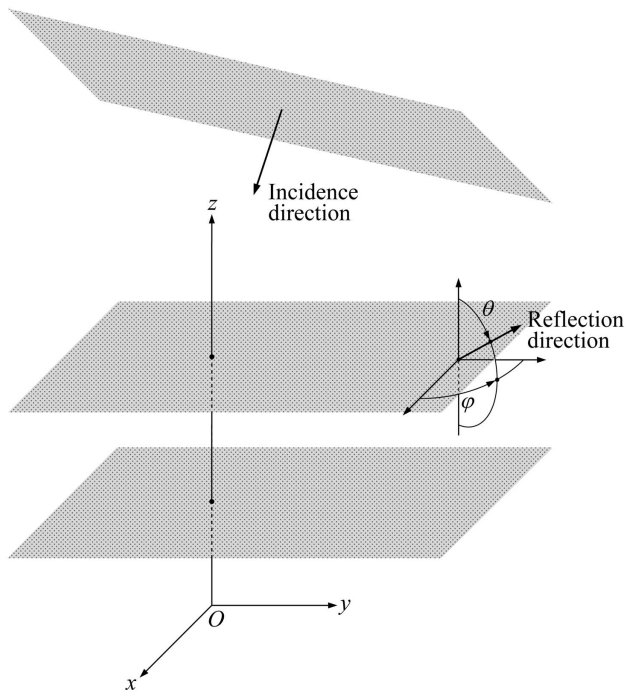


Fig. 1. Scattering geometry. A laterally infinite particulate layer is confined to the space between the two imaginary horizontal planes. The layer is illuminated from above by a plane electromagnetic wave.

(Fig. 1). To simplify the problem further, we will neglect the refracting/reflecting effects of the optical interfaces separating the interior of the layer and the surrounding space. This model does describe a cloud layer embedded in a gaseous atmosphere at wavelengths affected by molecular absorption, but is less realistic in application to particles inside water or ice bodies bounded by physical surfaces serving as optical interfaces. The specific discussion of the additional effects potentially exerted by the actual boundaries will be deferred to a forthcoming publication.

The resulting boundary-value problem has the standard mathematical structure [18,58] and can be addressed using a variety of existing computer solvers of the conventional vector RTE [3,15,57]. The single-scattering quantities entering the generalized RTE [52] are computed by assuming that the particles are homogeneous spheres and using the Lorenz—Mie computer program described in [53,54].

Consistent with [52,53], we imply the $\exp(-i\omega t)$ time-harmonic dependence of all electromagnetic fields, where $i = (-1)^{1/2}$, ω is the angular frequency, and t is time. For simplicity, we assume that all particles are made of the same material. The wave numbers of the host and the scattering particles are given, respectively, by

$$k_1 = k'_1 + ik''_1 \quad (1)$$

and

$$k_2 = k'_2 + ik''_2, \quad (2)$$

where $k'_1 > 0$, $k''_1 \geq 0$, $k'_2 > 0$, and $k''_2 \geq 0$. It is convenient to define the scattering problem in terms of the wavelength in a vacuum, λ , and the complex refractive indices of the host, m_1 , and the particles, m_2 , given, respectively, by

$$m_1 = m'_1 + im''_1 \quad (3)$$

and

$$m_2 = m'_2 + im''_2. \quad (4)$$

Then,

$$k_1 = \frac{2\pi m_1}{\lambda} = \frac{2\pi m'_1}{\lambda} + i \frac{2\pi m''_1}{\lambda} \quad (5)$$

and

$$k_2 = \frac{2\pi m_2}{\lambda} = \frac{2\pi m'_2}{\lambda} + i \frac{2\pi m''_2}{\lambda}. \quad (6)$$

We assume that the particulate slab of infinite lateral extent has a geometrical thickness Z and that the host material of the slab is perfectly homogeneous and thus does not scatter light (this includes neglecting Rayleigh scattering by air). The (purely absorption) vertical optical thickness of the host material $\mathcal{T}_{\text{host}}$ is given by

$$\mathcal{T}_{\text{host}} = 2Zk''_1 = \frac{4\pi Zm''_1}{\lambda}. \quad (7)$$

If $\mathcal{T}_{\text{host}}$ rather than m''_1 serves as a primary input parameter, then

$$k''_1 = \frac{\mathcal{T}_{\text{host}}}{2Z} \quad (8)$$

and

$$m''_1 = \frac{\mathcal{T}_{\text{host}}\lambda}{4\pi Z}. \quad (9)$$

We parameterize the dispersion of radii of polydisperse spherical particles by the standard gamma distribution [3,53] with specific effective radius r_{eff} and effective variance v_{eff} . Let n_0 be the number of particles per unit volume. Then the total vertical optical thickness of the particulate slab is

$$\mathcal{T} = \mathcal{T}_{\text{host}} + \mathcal{T}_{\text{particles}}, \quad (10)$$

where

$$\mathcal{T}_{\text{particles}} = Zn_0 C_{\text{ext}} \quad (11)$$

is the particulate optical thickness, and C_{ext} is the average extinction cross section per particle.

Two more quantities that enter the generalized vector RTE [52] are the normalized Stokes phase matrix, parameterized in terms of the so-called Wigner expansion coefficients α_p^s ($p = 1, 2, 3, 4$) and β_p^s ($p = 1, 2$), and the effective single-scattering albedo

$$\omega^{\text{eff}} = \frac{C_{\text{sca}}^{\text{eff}}}{2n_0^{-1}k''_1 + C_{\text{ext}}}, \quad (12)$$

where $C_{\text{sca}}^{\text{eff}}$ is the effective scattering cross section per particle.

All relevant polarimetric definitions and geometrical conventions of the vector radiative transfer theory can be found in [3,15,18,21]. The diffuse reflection properties of the particulate layer are parameterized in terms of the real-valued 4×4 so-called Stokes reflection matrix $\mathbf{R}(\mu, \mu_0, \varphi, \varphi_0)$, where μ is the cosine of the polar angle of the reflection direction θ measured from the positive z axis; μ_0 is minus the cosine of the polar angle of the incidence direction measured from the positive z axis; φ is the azimuth angle of the reflection direction

measured clockwise from the positive x axis; and φ_0 is the azimuth angle of the incidence direction measured clockwise from the positive x axis (Fig. 1). The definition of the reflection matrix is as follows:

$$\tilde{\mathbf{I}} = \frac{1}{\pi} \mu_0 \mathbf{R}(\mu, \mu_0, \varphi, \varphi_0) \mathbf{I}, \quad (13)$$

where $\tilde{\mathbf{I}}$ is the specific intensity column vector of the diffusely reflected light, and \mathbf{I} is the Stokes column vector of the incident plane electromagnetic wave [3,15,18]. For simplicity, we assume hereafter that $\mu_0 = 1$ (normal incidence) and $\varphi_0 = 0$.

The resulting computational scheme involves the following seven basic steps:

- (1a) specification of $m'_1, m''_1, m'_2, m''_2, \lambda$, and Z followed by computation of $\mathcal{T}_{\text{host}}$ according to Eq. (7) or, alternatively,
- (1b) specification of $m'_1, m'_2, m''_2, \lambda, Z$, and $\mathcal{T}_{\text{host}}$ followed by calculation of m''_1 according to Eq. (9);
- (2) specification of r_{eff} and v_{eff} ;
- (3) computation of $C_{\text{ext}}, C_{\text{sca}}^{\text{eff}}, \alpha_p^s$ ($p = 1, 2, 3, 4$), and β_p^s ($p = 1, 2$) [53];
- (4a) specification of n_0 or, alternatively,
- (4b) specification of the fraction f of the volume occupied by the particles followed by computation of n_0 according to $n_0 = f/\langle V \rangle$, where $\langle V \rangle$ is the average particle volume computed for the specific r_{eff} and v_{eff} ;
- (5) computation of ϖ^{eff} according to Eq. (12);
- (6) computation of \mathcal{T} according to Eqs. (10) and (11); and
- (7) computation of the reflection matrix \mathbf{R} by solving the vector RTE.

This computational scheme (hereinafter scheme A) is based on the first-principles theory of light scattering by particles immersed in an absorbing host. Besides using this scheme, we will also use the conventional heuristic scheme (hereinafter scheme B), which is different in that $C_{\text{ext}}, C_{\text{sca}}^{\text{eff}}, \alpha_p^s$ ($p = 1, 2, 3, 4$), and β_p^s ($p = 1, 2$) (step 3) are computed by using the conventional Lorenz—Mie theory based on the assumption that $m''_1 \equiv 0$. This will enable us to estimate typical errors caused by the use of the traditional approach to light scattering and radiative transfer.

3. PARTICLES IN ABSORBING GASEOUS ATMOSPHERE

We first consider the case of aerosol and cloud particles imbedded in an absorbing gaseous atmosphere. To parameterize this scenario, we use version (b) of step 1 and version (a) of step 4 of the numerical scheme summarized in the preceding section. Model 1 represents a layer of submicrometer-sized sulfate aerosols with $\mathcal{T}_{\text{particles}} \approx 0.9$ and is specified by the following parameters: $\lambda = 0.76 \mu\text{m}$, $m'_1 = 1$, $m'_2 = 1.42$, $m''_2 = 0$, $r_{\text{eff}} = 0.5 \mu\text{m}$, $v_{\text{eff}} = 0.1$, $n_0 = 0.5 \times 10^9 \text{ m}^{-3}$, and $Z = 1 \text{ km}$. Note that this wavelength is close to the center of the strong oxygen A-band. Model 2 represents an optically thick ($\mathcal{T}_{\text{particles}} \approx 10$) layer of 10 micrometer-sized water-cloud droplets and is specified by the following parameters: $\lambda = 1.35 \mu\text{m}$, $m'_1 = 1$, $m'_2 = 1.322$, $m''_2 = 1.06 \times 10^{-4}$, $r_{\text{eff}} = 10 \mu\text{m}$, $v_{\text{eff}} = 0.1$, $n_0 = 10^7 \text{ m}^{-3}$, and $Z = 2 \text{ km}$. In this case, the wavelength is close to the center of a strong water-vapor absorption band.

Table 1. Optical Properties of Model 1 According to Scheme A

$\mathcal{T}_{\text{host}}$	m''_1	\mathcal{T}	$C_{\text{sca}}^{\text{eff}}, \mu\text{m}^2$	$C_{\text{ext}}, \mu\text{m}^2$	ϖ^{eff}
0.1	0.60479×10^{-11}	1.02468	1.8494	1.8494	0.90241
1	0.60479×10^{-10}	1.92468	1.8494	1.8494	0.48043
3	0.18144×10^{-9}	3.92468	1.8494	1.8494	0.23561
10	0.60479×10^{-9}	10.9247	1.8494	1.8494	0.084641

Table 2. Optical Properties of Model 1 According to Scheme B

$\mathcal{T}_{\text{host}}$	m''_1	\mathcal{T}	$C_{\text{sca}}^{\text{eff}}, \mu\text{m}^2$	$C_{\text{ext}}, \mu\text{m}^2$	ϖ^{eff}
0.1	0	1.02468	1.8494	1.8494	0.90241
1	0	1.92468	1.8494	1.8494	0.48043
3	0	3.92468	1.8494	1.8494	0.23561
10	0	10.9247	1.8494	1.8494	0.084641

Tables 1 and 2 display the optical properties of model 1 computed using the first-principles scheme A and the conventional scheme B. It is obvious that all numbers agree to all decimal places shown. We have also computed the maximal differences between the corresponding elements of the effective single-scattering matrix [53]

$$\mathbf{F}(\Theta) = \begin{bmatrix} F_{11}(\Theta) & F_{21}(\Theta) & 0 & 0 \\ F_{21}(\Theta) & F_{11}(\Theta) & 0 & 0 \\ 0 & 0 & F_{33}(\Theta) & F_{34}(\Theta) \\ 0 & 0 & -F_{34}(\Theta) & F_{33}(\Theta) \end{bmatrix}, \quad (14)$$

where $\Theta \in [0, \pi]$ is the scattering angle. Again, the agreement is nearly perfect (relative differences less than 10^{-6} in the absolute-value sense for all Θ). This conclusion is not surprising given the extremely small resulting values of m''_1 in Table 1 even for $\mathcal{T}_{\text{host}}$ values as large as 10.

Tables 3 and 4 display the corresponding results for model 2, again computed using schemes A and B. As before, all numbers agree to all decimal places shown, and, furthermore, the elements of the scattering matrix agree to at least six significant decimal places. This agreement can again be traced to very small m''_1 values in Table 3 even for extreme values of $\mathcal{T}_{\text{host}}$.

The near-perfect agreement of the scheme A and B results serving as input to radiative-transfer computations implies that the corresponding solutions of the RTE (not shown) are also virtually identical. We can thus conclude that in the case of aerosol and cloud particles suspended in an absorbing gaseous atmosphere, the standard computational scheme based on the

Table 3. Optical Properties of Model 2 According to Scheme A

$\mathcal{T}_{\text{host}}$	m''_1	\mathcal{T}	$C_{\text{sca}}^{\text{eff}}, \mu\text{m}^2$	$C_{\text{ext}}, \mu\text{m}^2$	ϖ^{eff}
1	0.53715×10^{-10}	10.8030	485.60	490.15	0.89901
10	0.53715×10^{-9}	19.8030	485.60	490.15	0.49043
30	0.16114×10^{-8}	39.8030	485.60	490.15	0.24400
100	0.53715×10^{-8}	109.803	485.60	490.15	0.088449

Table 4. Optical Properties of Model 2 According to Scheme B

$\mathcal{T}_{\text{host}}$	m_1''	\mathcal{T}	$C_{\text{sca}}^{\text{eff}}, \mu\text{m}^2$	$C_{\text{ext}}, \mu\text{m}^2$	ϖ^{eff}
1	0	10.8030	485.60	490.15	0.89901
10	0	19.8030	485.60	490.15	0.49043
30	0	39.8030	485.60	490.15	0.24400
100	0	109.803	485.60	490.15	0.088449

assumption that $m_1'' \equiv 0$ provides accuracy quite sufficient for practical applications.

4. AIR BUBBLES IN WATER

We now use version (a) of step 1 and version (b) of step 4 of the computational scheme summarized in Section 2 and consider the case of air bubbles suspended in a semi-infinite ($Z = \infty$) layer of water. Implicitly, $\mathcal{T} = \mathcal{T}_{\text{host}} = \mathcal{T}_{\text{particles}} = \infty$. Model 3 is specified by the following parameters: $m_2' = 1$, $m_2'' = 0$, $r_{\text{eff}} = 10 \mu\text{m}$, $v_{\text{eff}} = 0.05$, and $f = 0.002$ and 0.02 . The wavelengths and the corresponding values of m_1 are listed in Table 5. Note that the volume fraction $f = 0.002$ is definitely small enough to make the RTE applicable, while $f = 0.02$ still

Table 5. Optical Properties of Model 3

$\lambda,$ μm	m_1'	m_1''	$C_{\text{ext,A}},$ μm^2	$C_{\text{ext,B}},$ μm^2	$C_{\text{sca,A}}^{\text{eff}},$ μm^2	$C_{\text{sca,B}}^{\text{eff}},$ μm^2
0.6	1.332	1.09×10^{-8}	547.7852	547.7852	547.7860	547.7852
1	1.327	2.89×10^{-6}	549.2962	549.2962	549.4270	549.2962
1.4	1.321	1.38×10^{-4}	549.6329	549.6346	554.1468	549.6346
2	1.306	1.1×10^{-3}	546.5237	546.6039	572.9135	546.6039
2.7	1.188	0.019	462.6561	488.9096	1183.768	488.9096
3.3	1.450	0.0368	548.8644	551.1966	2682.243	551.1966

appears to be sufficiently small to make RTE predictions reasonably accurate [59,60].

Table 5 also compares the corresponding extinction and effective scattering cross sections computed according to schemes A (subscript A) and B (subscript B). The corresponding f -dependent effective single-scattering albedos are compared in Table 6. It is seen that the errors of the traditional approach (scheme B) become substantial at the longest wavelengths with large m_1'' . The same is true of the phase function $F_{11}(\Theta)$ and the degree of linear polarization for unpolarized incident light $-F_{21}(\Theta)/F_{11}(\Theta)$ shown in Fig. 2. Consistent with Eq. (12), increasing the particle volume fraction always serves to increase the effective single-scattering albedo. Also, the scheme A values of $C_{\text{sca}}^{\text{eff}}$ and ϖ^{eff} are always greater than the respective scheme B values, the differences becoming quite dramatic at the two longest wavelengths.

Figures 3 and 4 show the corresponding results of vector radiative-transfer computations. Specifically, Fig. 3 depicts the (1,1) element of the reflection matrix $R_{11}(\mu, \mu_0 = 1, \varphi = 0, \varphi_0 = 0)$, traditionally called the reflection coefficient, while

Table 6. Effective Single-Scattering Albedo of Model 3

$\lambda, \mu\text{m}$	f	ϖ_A^{eff}	ϖ_B^{eff}
0.6	0.002	0.99926	0.99925
	0.02	0.99993	0.99993
1.0	0.002	0.89435	0.89414
	0.02	0.98853	0.98830
1.4	0.002	0.20022	0.19858
	0.02	0.71832	0.71247
2.0	0.002	0.044333	0.042297
	0.02	0.32111	0.30635
2.7	0.002	0.0074538	0.0030780
	0.02	0.072633	0.029950
3.3	0.002	0.010665	0.0021917
	0.02	0.10460	0.021493

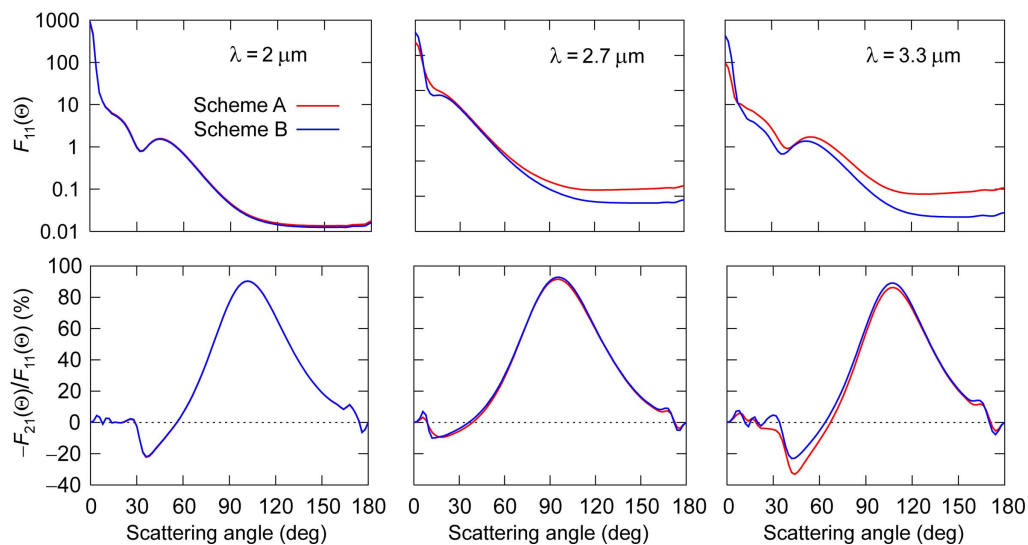


Fig. 2. Single-scattering phase function (upper panels) and the degree of linear polarization (lower panels) computed for model 3 using schemes A (red curves) and B (blue curves). At the three shorter wavelengths listed in Table 5, the scheme A and B results (not shown) are virtually indistinguishable.

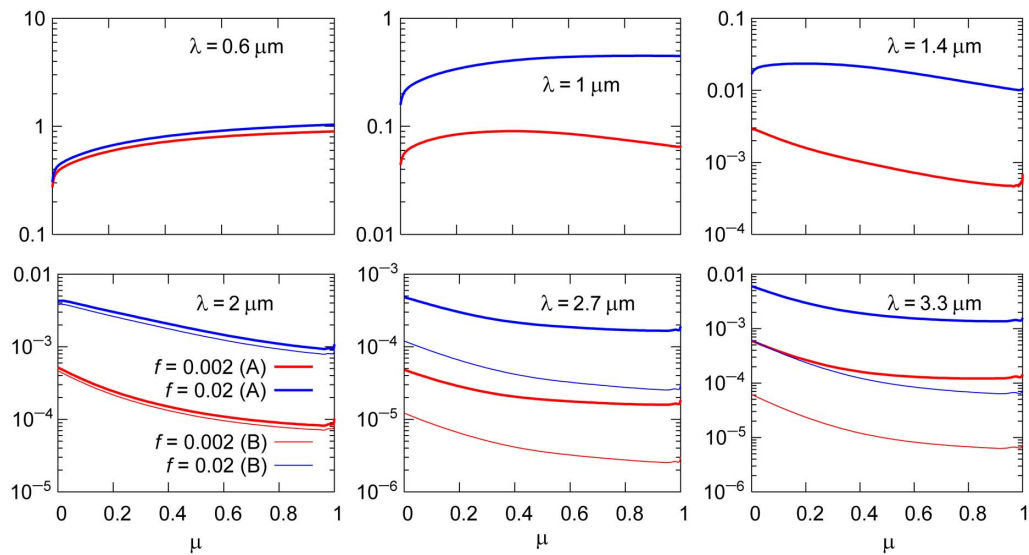


Fig. 3. Reflection coefficient for model 3 computed using schemes A and B. The results are shown for six wavelengths and two values of the particle volume fraction. The scheme A and B results in the upper three panels are virtually indistinguishable.

Fig. 4 shows the degree of linear polarization for unpolarized incident light given by the ratio

$$P(\mu) = -\frac{R_{21}(\mu, \mu_0 = 1, \varphi = 0, \varphi_0 = 0)}{R_{11}(\mu, \mu_0 = 1, \varphi = 0, \varphi_0 = 0)}. \quad (15)$$

Figure 3 reveals that the $f = 0.02$ reflectances are always greater than their $f = 0.002$ counterparts, which is consistent with the above-noted trait of the effective single-scattering albedo. At the shortest wavelength (upper left panel), the contribution of multiply scattered light is so large that as small a difference as 0.00067 in ϖ^{eff} causes noticeable differences

between the blue and red curves. At longer wavelengths, these differences become much larger.

The scheme A and B curves in the upper three panels of Fig. 3 are essentially indistinguishable. However, the relative differences between the respective thick and thin curves become noticeable at $\lambda = 2 \mu\text{m}$ and quite significant at the two longest wavelengths. This, no doubt, is the result of the large single-scattering albedo differences in Table 6 and the growing phase-function differences in Fig. 2.

However, while there are order-of-magnitude differences between the scheme A and B reflectances at $\lambda = 2.7$ and $3.3 \mu\text{m}$, the reflectances themselves are very small owing to strong absorption in the water host. We can thus conclude that the

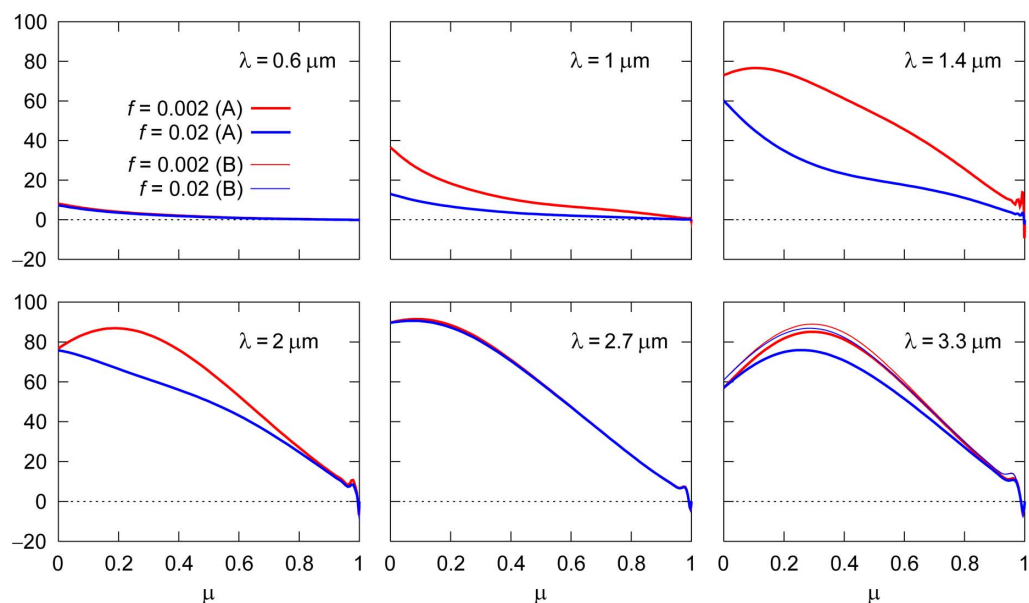


Fig. 4. Degree of linear polarization $P(\mu)$ (%) for model 3 computed using schemes A and B. The results are shown for six wavelengths and two values of the particle volume fraction. Scheme B results are shown only for $\lambda = 3.3 \mu\text{m}$, since at other wavelengths, they are hardly distinguishable from the respective scheme A results.

traditional scheme B can often be used unless accurate estimates of very low (less than $\sim 1\%$) reflectances are required.

Figure 4 shows that the $f = 0.002$ polarization is in most cases greater than its $f = 0.02$ counterpart. This is consistent with the definition (15) and the f -dependence of the reflection coefficient. The scheme A and B differences in polarization are small if not negligible.

5. CONCLUDING REMARKS

Our primary objective in this paper was to analyze errors caused by using the traditional radiative-transfer approach wherein the single-scattering properties of particles are calculated assuming that the host medium is nonabsorbing. It was clear from the outset that on one hand, the effects of absorption in the host medium on the single-scattering input to the RTE would increase with m_1'' . On the other hand, it could also be expected that strong absorption suppresses multiple scattering and thereby can potentially make the resulting reflectance too small to be of practical interest. It was therefore important to analyze whether there are situations wherein m_1'' is not large enough to eradicate all observable manifestations of multiple scattering and yet is sufficiently large to cause detectable differences between the results of applying the first-principles scheme A and the conventional heuristic scheme B detailed in Section 2.

We have shown that in the case of aerosol and cloud particles suspended in a gaseous planetary atmosphere, even extreme values of the host absorption optical thickness yield very small values of m_1'' . As a consequence, the traditional scheme has been found to produce excellent single-scattering and, by implication, multiple-scattering results. Thus, there is no need to modify the existing traditional tools developed for modeling atmospheric radiation. There is no doubt that this conclusion will be gladly received by the practitioners of atmospheric radiative transfer.

In the case of water as the host medium, the m_1'' values can be much larger and can affect much stronger the single-scattering properties of the embedded particles. In such cases the traditional scheme B was indeed found to generate noticeable to very large relative errors in the reflection coefficient. Yet the resulting reflectance itself is very small to the point of being useless in many practical applications. The errors of the traditional scheme in the degree of linear polarization of the diffusely reflected light are significantly smaller and can often be ignored.

Funding. National Aeronautics and Space Administration (NASA).

Acknowledgment. We thank two anonymous reviewers for their positive evaluation of the initial paper and constructive comments.

REFERENCES

- H. C. van de Hulst, *Light Scattering by Small Particles* (Wiley, 1957).
- M. Kerker, *The Scattering of Light and Other Electromagnetic Radiation* (Academic, 1969).
- J. E. Hansen and L. D. Travis, "Light scattering in planetary atmospheres," *Space Sci. Rev.* **16**, 527–610 (1974).
- V. V. Sobolev, *Light Scattering in Planetary Atmospheres* (Pergamon, 1975).
- A. Ishimaru, *Wave Propagation and Scattering in Random Media* (Academic, 1978).
- H. C. van de Hulst, *Multiple Light Scattering: Tables, Formulas, and Applications* (Academic, 1980), Vols. 1 and 2.
- R. G. Newton, *Scattering Theory of Waves and Particles* (Springer, 1982).
- C. F. Bohren and D. R. Huffman, *Absorption and Scattering of Light by Small Particles* (Wiley, 1983).
- L. Tsang, J. A. Kong, and R. T. Shin, *Theory of Microwave Remote Sensing* (Wiley, 1985).
- R. M. Goody and Y. L. Yung, *Atmospheric Radiation: Theoretical Basis* (Oxford, 1989).
- E. G. Yanovitskij, *Light Scattering in Inhomogeneous Atmospheres* (Springer, 1997).
- M. I. Mishchenko, J. W. Hovenier, and L. D. Travis, eds., *Light Scattering by Nonspherical Particles: Theory, Measurements, and Applications* (Academic, 2000).
- K. N. Liou, *An Introduction to Atmospheric Radiation* (Academic, 2002).
- M. I. Mishchenko, L. D. Travis, and A. A. Lacis, *Scattering, Absorption, and Emission of Light by Small Particles* (Cambridge University, 2002).
- J. W. Hovenier, C. van der Mee, and H. Domke, *Transfer of Polarized Light in Planetary Atmospheres—Basic Concepts and Practical Methods* (Springer, 2004).
- A. Doicu, T. Wriedt, and Y. A. Eremin, *Light Scattering by Systems of Particles* (Springer, 2006).
- P. A. Martin, *Multiple Scattering: Interaction of Time-Harmonic Waves with N Obstacles* (Cambridge University, 2006).
- M. I. Mishchenko, L. D. Travis, and A. A. Lacis, *Multiple Scattering of Light by Particles: Radiative Transfer and Coherent Backscattering* (Cambridge University, 2006).
- F. Borghese, P. Denti, and R. Saija, *Scattering from Model Nonspherical Particles. Theory and Applications to Environmental Physics* (Springer, 2007).
- M. Wendisch and P. Yang, *Theory of Atmospheric Radiative Transfer* (Wiley-VCH, 2012).
- M. I. Mishchenko, *Electromagnetic Scattering by Particles and Particle Groups: An Introduction* (Cambridge University, 2014).
- G. Kristensson, *Scattering of Electromagnetic Waves by Obstacles* (Scitech Publishing, 2016).
- K.-N. Liou and P. Yang, *Light Scattering by Ice Crystals: Fundamentals and Applications* (Cambridge, 2016).
- G. Gouesbet and G. Gréhan, *Generalized Lorenz—Mie Theories* (Springer, 2017).
- M. Loewen, "Inside whitecaps," *Nature* **418**, 830 (2002).
- G. H. Hale and M. R. Query, "Optical constants of water in the 200-nm to 200- μm wavelength region," *Appl. Opt.* **12**, 555–563 (1973).
- S. G. Warren and R. E. Brandt, "Optical constants of ice from the ultraviolet to the microwave: a revised compilation," *J. Geophys. Res.* **113**, D14220 (2008).
- J. A. Stratton, *Electromagnetic Theory* (McGraw-Hill, 1941).
- W. C. Mundy, J. A. Roux, and A. M. Smith, "Mie scattering by spheres in an absorbing medium," *J. Opt. Soc. Am.* **64**, 1593–1597 (1974).
- P. Chýlek, "Light scattering by small particles in an absorbing medium," *J. Opt. Soc. Am.* **67**, 561–563 (1977).
- C. F. Bohren and D. P. Gilra, "Extinction by a spherical particle in an absorbing medium," *J. Colloid Interface Sci.* **72**, 215–221 (1979).
- P. Bruscaioni, A. Ismaelli, and G. Zaccanti, "A note on the definition of scattering cross sections and phase functions for spheres immersed in an absorbing medium," *Waves Random Media* **3**, 147–156 (1993).
- M. Quinten and J. Rostalski, "Lorenz—Mie theory for spheres immersed in an absorbing host medium," *Part. Part. Syst. Charact.* **13**, 89–96 (1996).
- A. N. Lebedev, M. Gratz, U. Kreibig, and O. Stenzel, "Optical extinction by spherical particles in an absorbing medium: application to composite absorbing films," *Eur. Phys. J. D* **6**, 365–369 (1999).

35. W. Sudiarta and P. Chylek, "Mie-scattering formalism for spherical particles embedded in an absorbing medium," *J. Opt. Soc. Am. A* **18**, 1275–1278 (2001).
36. W. Sudiarta and P. Chylek, "Mie scattering efficiency of a large spherical particle embedded in an absorbing medium," *J. Quant. Spectrosc. Radiat. Transfer* **70**, 709–714 (2001).
37. P. Yang, B.-C. Gao, W. J. Wiscombe, M. I. Mishchenko, S. E. Platnick, H.-L. Huang, B. A. Baum, Y. X. Hu, D. M. Winker, S.-C. Tsay, and S. K. Park, "Inherent and apparent scattering properties of coated or uncoated spheres embedded in an absorbing host medium," *Appl. Opt.* **41**, 2740–2759 (2002).
38. G. Videen and W. Sun, "Yet another look at light scattering from particles in absorbing media," *Appl. Opt.* **42**, 6724–6727 (2003).
39. W. Sun, N. G. Loeb, and Q. Fu, "Light scattering by a coated sphere immersed in absorbing medium: a comparison between the FDTD and analytic solutions," *J. Quant. Spectrosc. Radiat. Transfer* **83**, 483–492 (2004).
40. Q. Fu and W. Sun, "Apparent optical properties of spherical particles in absorbing medium," *J. Quant. Spectrosc. Radiat. Transfer* **100**, 137–142 (2006).
41. J. Randrianalisoa, D. Baillis, and L. Pilon, "Modeling radiation characteristics of semitransparent media containing bubbles or particles," *J. Opt. Soc. Am. A* **23**, 1645–1656 (2006).
42. J. Yin and L. Pilon, "Efficiency factors and radiation characteristics of spherical scatterers in an absorbing medium," *J. Opt. Soc. Am. A* **23**, 2784–2796 (2006).
43. J. R. Frisvad, N. J. Christensen, and H. W. Jensen, "Computing the scattering properties of participating media using Lorenz–Mie theory," *ACM Trans. Graph.* **26**, 60 (2007).
44. S. Durant, O. Calvo-Perez, N. Vukadinovic, and J.-J. Greffet, "Light scattering by a random distribution of particles embedded in absorbing media: diagrammatic expansion of the extinction coefficient," *J. Opt. Soc. Am. A* **24**, 2943–2952 (2007).
45. S. Durant, O. Calvo-Perez, N. Vukadinovic, and J.-J. Greffet, "Light scattering by a random distribution of particles embedded in absorbing media: full-wave Monte Carlo solutions of the extinction coefficient," *J. Opt. Soc. Am. A* **24**, 2953–2962 (2007).
46. L. A. Dombrovsky and D. Baillis, *Thermal Radiation in Disperse Systems: An Engineering Approach* (Begell House, 2010).
47. R. Ceolato, N. Riviere, M. J. Berg, and B. Biscans, "Electromagnetic scattering from aggregates embedded in absorbing media," in *Progress In Electromagnetics Research Symposium Proceedings, Taipei* (2013), pp. 717–721.
48. B. Aernouts, R. Watté, R. van Beers, F. Delport, M. Merchiers, J. de Block, J. Lammertyn, and W. Saeys, "Flexible tool for simulating the bulk optical properties of polydisperse spherical particles in an absorbing host: experimental validation," *Opt. Express* **22**, 20223–20238 (2014).
49. L. X. Ma, B. W. Xie, C. C. Wang, and L. H. Liu, "Radiative transfer in dispersed media: considering the effect of host medium absorption on particle scattering," *J. Quant. Spectrosc. Radiat. Transfer* **230**, 24–35 (2019).
50. M. I. Mishchenko, "Electromagnetic scattering by a fixed finite object embedded in an absorbing medium," *Opt. Express* **15**, 13188–13202 (2007).
51. M. I. Mishchenko, "Multiple scattering by particles embedded in an absorbing medium. 1. Foldy-Lax equations, order-of-scattering expansion, and coherent field," *Opt. Express* **16**, 2288–2301 (2008).
52. M. I. Mishchenko, "Multiple scattering by particles embedded in an absorbing medium. 2. Radiative transfer equation," *J. Quant. Spectrosc. Radiat. Transfer* **109**, 2386–2390 (2008).
53. M. I. Mishchenko and P. Yang, "Far-field Lorenz–Mie scattering in an absorbing host medium: theoretical formalism and FORTRAN program," *J. Quant. Spectrosc. Radiat. Transfer* **205**, 241–252 (2018).
54. M. I. Mishchenko, J. M. Dlugach, J. A. Lock, and M. A. Yurkin, "Far-field Lorenz–Mie scattering in an absorbing host medium. II: Improved stability of the numerical algorithm," *J. Quant. Spectrosc. Radiat. Transfer* **217**, 274–277 (2018).
55. M. I. Mishchenko, G. Videen, and P. Yang, "Extinction by a homogeneous spherical particle in an absorbing medium," *Opt. Lett.* **42**, 4873–4876 (2017).
56. M. I. Mishchenko and J. M. Dlugach, "Scattering and extinction by spherical particles immersed in an absorbing host medium," *J. Quant. Spectrosc. Radiat. Transfer* **211**, 179–187 (2018).
57. M. I. Mishchenko, J. M. Dlugach, J. Chowdhary, and N. T. Zakharova, "Polarized bidirectional reflectance of optically thick sparse particulate layers: an efficient numerically exact radiative-transfer solution," *J. Quant. Spectrosc. Radiat. Transfer* **156**, 97–108 (2015).
58. J. Lenoble, *Radiative Transfer in Scattering and Absorbing Atmospheres: Standard Computational Procedures* (A. Deepak Publishing, 1985).
59. K. Muinonen, M. I. Mishchenko, J. M. Dlugach, E. Zubko, A. Penttilä, and G. Videen, "Coherent backscattering verified numerically for a finite volume of spherical particles," *Astrophys. J.* **760**, 118 (2012).
60. M. I. Mishchenko, D. Goldstein, J. Chowdhary, and A. Lompado, "Radiative transfer theory verified by controlled laboratory experiments," *Opt. Lett.* **38**, 3522–3525 (2013).